

JGR Atmospheres

RESEARCH ARTICLE

10.1029/2020JD034327

Key Points:

- Between 1978 and 2019, the global annual mean sulfuryl fluoride mole fraction in the atmosphere increased from 0.3 ± 0.02 to 2.5 ± 0.08 ppt
- Between 1978 and 2019, global emissions, as inferred from atmospheric measurements, increased from 0.5 ± 0.4 Gg yr⁻¹ to 2.9 ± 0.4 Gg yr⁻¹
- The global emissions increase is driven by the SO₂F₂ growing use in structural fumigation in North America and in grain treatment worldwide

Supporting Information:

Supporting Information may be found in the online version of this article.

Correspondence to:

A. Gressent,
agressen@mit.edu

Citation:

Gressent, A., Rigby, M., Ganesan, A. L., Prinn, R. G., Manning, A. J., Mühle, J., et al. (2021). Growing atmospheric emissions of sulfuryl fluoride. *Journal of Geophysical Research: Atmospheres*, 126, e2020JD034327. <https://doi.org/10.1029/2020JD034327>

Received 28 NOV 2020

Accepted 20 APR 2021

Author Contributions:













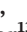



Conceptualization: M. Rigby

Data curation: A. L. Ganesan, A. J. Manning, J. Mühle, P. K. Salameh, P. B. Krummel, P. J. Fraser, L. P. Steele, B. Mitrevski, R. F. Weiss, C. M. Harth, R. H. Wang, S. O'Doherty, D. Young, S. Park, S. Li, B. Yao, S. Reimann, M. K. Vollmer, M. Maione, J. Arduini, C. R. Lunder

Formal analysis: M. Rigby, A. L. Ganesan, R. G. Prinn, A. J. Manning, J. Mühle, P. K. Salameh, P. B. Krummel, P. J. Fraser, L. P. Steele, B. Mitrevski, R. F. Weiss, S. O'Doherty, D. Young, S. Park, B. Yao, S. Reimann, M. K. Vollmer, J. Arduini

Funding acquisition: R. G. Prinn, P. K. Salameh

Growing Atmospheric Emissions of Sulfuryl Fluoride

A. Gressent¹ , M. Rigby² , A. L. Ganesan³ , R. G. Prinn¹ , A. J. Manning⁴ , J. Mühle⁵ , P. K. Salameh⁵, P. B. Krummel⁶ , P. J. Fraser⁶, L. P. Steele⁶ , B. Mitrevski⁶, R. F. Weiss⁵ , C. M. Harth⁵, R. H. Wang⁵ , S. O'Doherty² , D. Young³ , S. Park⁷ , S. Li⁸, B. Yao⁹ , S. Reimann¹⁰ , M. K. Vollmer¹⁰ , M. Maione^{11,12}, J. Arduini^{11,12}, and C. R. Lunder¹³

¹Center for Global Change Science, Massachusetts Institute of Technology, Cambridge, MA, USA, ²School of Chemistry, University of Bristol, Bristol, UK, ³School of Geographical Sciences, University of Bristol, Bristol, UK, ⁴Met Office, London, UK, ⁵Scripps Institution of Oceanography, University of California at San Diego, San Diego, CA, USA, ⁶Climate Science Centre, CSIRO Oceans and Atmosphere, Victoria, Aspendale, Australia, ⁷Department of Oceanography, College of Natural Science, Kyungpook National University, Daegu, South Korea, ⁸Climate Research Division, National Institute of Meteorological Sciences, Seogwipo, Korea, ⁹Meteorological Observation Center of China Meteorological Administration, Beijing, China, ¹⁰Laboratory for Air Pollution and Environmental Technology, Empa, Swiss Federal Laboratories for Materials Science and Technology, Dübendorf, Switzerland, ¹¹Department of Pure and Applied Sciences, University of Urbino, Urbino, Italy, ¹²Institute of Atmospheric Sciences and Climate, National Research Council, Bologna, Italy, ¹³Norwegian Institute for Air Research, Kjeller, Norway

Abstract The potent greenhouse gas sulfuryl fluoride (SO₂F₂) is increasingly used as a fumigant, replacing methyl bromide, whose structural and soil fumigation uses have been phased out under the Montreal Protocol. We use measurements on archived air samples and in situ observations from the Advanced Global Atmospheric Gases Experiment (AGAGE) and a box model of the global atmosphere to show a global increase of SO₂F₂ mole fraction from 0.3 ± 0.02 to 2.5 ± 0.08 ppt along with a global increase in emissions from 0.5 ± 0.4 Gg yr⁻¹ to 2.9 ± 0.4 Gg yr⁻¹ from 1978 to 2019. Based on a hybrid model incorporating bottom-up industry data and a top-down downscaling approach, we estimate the spatial distribution and trend in SO₂F₂ regional emissions between 2000 and 2019 and propose that the global emissions increase is driven by the growing use of SO₂F₂ in structural fumigation in North America and in postharvest treatment of grains and other agricultural products worldwide.

Plain Language Summary Sulfuryl fluoride (SO₂F₂) is a potent greenhouse gas that has been used increasingly in fumigation since the global phase-down in the nonquarantine/preshipment use of methyl bromide under the Montreal Protocol. Despite its potential to warm the climate, there is great uncertainty surrounding the magnitude and location of SO₂F₂ emissions, which limits our ability to target emissions mitigation measures. We have used atmospheric observations from the Advanced Global Atmospheric Gases Experiment to show that global emissions increased from close to zero in the early 1980s to ~ 2.4 Gg yr⁻¹ in 2019. We find that the primary source of these global emissions in 2019 was structural fumigation in North America, but that the increase over the last two decades has also been driven by the growing use of SO₂F₂ in postharvest treatment of crops in many countries around the world.

1. Introduction

The use of synthetic chemical pesticides methyl bromide (CH₃Br) and sulfuryl fluoride (SO₂F₂) for the control of insects in stored agricultural products or for structural (building) fumigation is widespread in most developed and some developing countries. These chemicals are very toxic, and both are greenhouse gases (GHGs) influencing global climate. Methyl bromide, whose emissions have a substantial natural component, is also an ozone depleting substance (ODS), responsible for depletion of global stratospheric ozone (e.g., Engel & Rigby et al., 2018). As a consequence, fumigation (known as nonquarantine/preshipment [nonQPS]) uses of CH₃Br were phased out under the Montreal Protocol on substances that deplete the ozone layer (1998, <https://ozone.unep.org/treaties/montreal-protocol>, Methyl Bromide Technical Options Committee, MBTOC, 2014, 2018) resulting in a large decrease in its consumption (Carpenter & Reimann et al., 2014; Engel & Rigby et al., 2018). In response, SO₂F₂ has replaced CH₃Br in non-QPS applications and is now one of the main structural and postharvest fumigants of dried fruits, tree nuts, grains, and timbers.

Methodology: M. Rigby, A. L. Ganesan, R. G. Prinn, A. J. Manning, P. K. Salameh

Project Administration: R. G. Prinn, P. K. Salameh

Writing – original draft: M. Rigby, A. L. Ganesan, A. J. Manning

Writing – review & editing: M. Rigby, A. L. Ganesan, R. G. Prinn, A. J. Manning, J. Mühle, P. K. Salameh, P. B. Krummel, P. J. Fraser, L. P. Steele, B. Mitrevski, R. F. Weiss, C. M. Harth, R. H. Wang, S. O'Doherty, D. Young, S. Park, S. Li, B. Yao, S. Reimann, M. K. Vollmer, M. Maione, J. Arduini, C. R. Lunder

Although it does not have a direct impact on stratospheric ozone like its predecessor CH_3Br , SO_2F_2 is a potent greenhouse gas with a global warming potential (GWP) over a 100-year time horizon of $\sim 4,780$ (Papadimitriou et al., 2008). Its future emissions are expected to continue to increase significantly (MB-TOC, 2018). As reported in previous studies, the atmospheric removal of SO_2F_2 is mainly driven by hydrolysis in the surface ocean with a partial lifetime of 40 ± 13 years (Mühle et al., 2009) and by reaction with the hydroxyl radical (OH) with a partial lifetime of 300 years (Dillon et al., 2008; Papadimitriou et al., 2008), resulting in an overall atmospheric lifetime of 36 ± 11 years (Mühle et al., 2009). Mühle et al. (2009) also showed growth of SO_2F_2 mole fraction in the global atmosphere with a mean growth rate of $5 \pm 1\% \text{ yr}^{-1}$ from 1978 to 2007. They found that SO_2F_2 global total emissions were 0.6 Gg yr^{-1} in 1978, 1.1 Gg yr^{-1} in 1995, and 1.9 Gg yr^{-1} in 2007.

Here, we present an update of the global SO_2F_2 abundance and emissions for recent years and for the first time, a regional and sectoral breakdown of these emissions. These distributions are critical for understanding where and how this potent greenhouse gas is being used.

In Section 2, we present the top-down and bottom-up downscaling approaches that are used for global and regional emissions estimations, respectively. We present spatially distributed SO_2F_2 emissions for North America (USA, Canada, Mexico, Cuba, Trinidad and Tobago, Jamaica), Europe (Italy, Switzerland, Germany, France, UK, Belgium, Greece, Spain, Ireland, Portugal, The Netherlands, Sweden, Austria, Turkey), Asia (China, Japan, Vietnam, Thailand), Australia, and individual countries (Egypt, Indonesia), where bottom-up industrial data are available between 2000 and 2019. In Section 3, we discuss the Advanced Global Atmospheric Gases Experiment (AGAGE) in situ observation data used in this study. Section 4 focuses on the results and their interpretation. Finally, Section 5 summarizes and discusses the overall conclusions with some perspectives for future work.

2. Materials and Methods

2.1. Global Top-Down Emissions Estimation

The AGAGE 12-box model has been used previously to calculate the global mean growth rate and emissions of SO_2F_2 . The model box boundaries are defined by horizontal divisions at 30°N , 0° , and 30°S , and vertical divisions at 1,000, 500, 200, and 0 hPa (i.e., 12 boxes overall, 8 in the troposphere, 4 in the stratosphere, Cunnold et al., 1983; Mühle et al., 2009; Rigby et al., 2013). This formulation allows us to resolve background mole fractions measured in each semi-hemisphere with the model providing some information on processes such as (annually repeating) stratosphere-troposphere exchange and interhemispheric transport. As above, the steady-state lifetime of SO_2F_2 is estimated at 36 ± 11 years in the 12-box model, based on the 40-year partial lifetime with respect to ocean uptake (Mühle et al., 2009) and a more recent rate of reaction with OH (Burkholder et al., 2015). The rate of loss to the oceans is scaled in each surface semi-hemispheric box to provide the same relative loss rate as was estimated for carbon tetrachloride (Yvon-Lewis & Butler, 2002). This results in 33% of the oceanic loss occurring in the Northern Hemisphere (NH), and 67% in the Southern Hemisphere (SH), largely reflecting differences in oceanic surface area. While there may be differences in this scaling for SO_2F_2 , any associated errors in the global emissions presented below are expected to be small. The 12-box model OH concentration is based on 3D model fields from Spivakovsky et al. (2000), adjusted to match trends in AGAGE methyl chloroform (CH_3CCl_3) mole fractions (Rigby et al., 2013).

Monthly mean in situ AGAGE observations presented in Section 3 are used to constrain the model, after above-baseline “pollution events” have been removed from the data using a statistical filtering algorithm (following O'Doherty et al., 2001). The SO_2F_2 observations before 2004 are from archived air samples (as described in Mühle et al., 2009, their Section 2.3). Unlike Mühle et al. (2009), we have not used polynomial fits to the data as inputs to the inversion, but have instead used the actual data. In addition, we have prefiltered outliers from the archive tank record. For SO_2F_2 , due to the sparse NH data before in situ measurements started in the NH, the fits used for the iterative filtering are guided by the derived SH fit, shifted by 2 years (c.f. Mühle et al., 2019). This means that we are now more confident that the early NH archive samples are relatively free from contamination, and therefore several samples that were rejected in Mühle et al. (2009) were included here. In the inversion, we applied an uncertainty to each monthly mean or archive sample, which approximated the combined uncertainty due to both the measurement and model. For the in situ

data, this term was assumed to be equal to the observed monthly baseline variability (e.g., following Rigby et al., 2014). For the archive points, we used the measurement repeatability plus the mean monthly baseline variability in the same hemisphere during the period where in situ data were available, scaled by the mean mole fraction difference between the in situ and archive data.

To estimate emissions using the model and the data, we use a Bayesian method from Rigby et al. (2011, 2014). Briefly, this method does not rely on a priori estimates of absolute emissions magnitudes, but instead constrains only the expected year-to-year emissions variability. Following Rigby et al. (2011) and Engel & Rigby et al. (2018), we assume that, in the absence of observations, emissions change by 0 Gg yr^{-1} , $\pm 20\%$ of the maximum global emissions magnitude from the industrial estimate of Mühle et al. (2009). Essentially, this method provides a weak smoothing to the derived emissions, which is required where there are large gaps in the data, for example, during the period when data from archived air were used. The derived emissions were not found to be sensitive to reasonable changes in the a priori constraints. The uncertainties in the a posteriori emissions are determined by the measurement uncertainty and the magnitude of the prior constraint, and are augmented by a term related to the systematic lifetime and calibration scale uncertainties (following Rigby et al., 2014). The model calculations have been performed for global annual emissions from 1978 to 2019.

2.2. Regional Emissions Estimation

SO_2F_2 emissions are estimated for the two main sectors of emissions, structural fumigation and postharvest treatment (hereafter denoted SF and PT, respectively). Minor SO_2F_2 uses/emissions from plasma cleaning gas in semiconductor production (Hobbs & Hart, 2004), as a cover gas in magnesium production replacing sulfur hexafluoride (SF_6 , Mühle et al., 2009), and minor production from electrical discharge decomposition of SF_6 in transformers (Kóréh et al., 1997) are not considered here due to their relatively small contributions.

Regional emissions estimation using traditional inverse methods of atmospheric data (e.g., Fang et al., 2019; Rigby et al., 2019; Say et al., 2019) are challenging for SO_2F_2 due to very sporadic (frequency of hours) emissions from fumigation and the difficulty for models to capture this type of signal. We thus estimate emissions for the SF and PT sectors using a downscaling approach of the global emissions to regional scales. We estimate emissions for the years 2000–2019, inclusive, for the continental regions of North America (USA, Canada, Mexico, Cuba, Trinidad and Tobago, Jamaica), Europe (Italy, Switzerland, Germany, France, UK, Belgium, Greece, Spain, Ireland, Portugal, The Netherlands, Sweden, Austria, Turkey), Asia (China, Japan, Vietnam, Thailand), Australia, and for individual countries (Egypt, Indonesia) where SO_2F_2 use and emissions reports are the most readily available (details in the Supporting Information S1). Since emissions or consumption reports are not available for all countries that use SO_2F_2 , we use our downscaling of the global top-down emissions by region and sector that merges consumption reports and various proxy data.

The most important variables to consider are the year when the fumigant use began and the partitioning of the country's total emissions between SF and PT (Table 1). These are taken from MBTOC (2006, 2010, 2014, 2018), Buckley and Thoms (2012), Dow AgroSciences (2010, 2011), Prabhakaran et al. (2006), Dunse et al. (2019, which provide the Australian SO_2F_2 imports, consumption and emissions data), Cao et al. (2014), Widayanti et al. (2016), and Schwarz et al. (2011, which provides a review of regulation on certain fluorinated greenhouse gases). The first countries to use SO_2F_2 were the USA and Japan for structural fumigation. This occurred before the 2000s and their SF emission partitions are estimated as 95% and 100%, respectively. In Europe, Australia, China and the other countries where the gas has been licensed (MBTOC, 2006, 2010, 2014, 2018) SO_2F_2 is used predominantly for PT. In order to determine the partitioning of the country's total emissions between SF and PT, we assume that if the SO_2F_2 registration is only reported for SF then the partitioning is 100% for SF and 0% for PT (and vice versa). In the case where SO_2F_2 is registered for both SF and PT and we know from the literature that the main SO_2F_2 source is SF, for example, then we allocate a large fraction to the SF sector that is, 95%, and a small fraction to the PT sector that is, 5% (and vice versa).

Emissions estimates on the regional scale rely on several proxies. First, the spatial distribution of the emissions is defined yearly for the SF and PT sectors as detailed in Equations 1 and 2, respectively.

Table 1

The Year in Which SO₂F₂ Began to be Used and the Partitioning of the Country's Total Emissions Between SF and PT Sectors, Based on Dunse et al. (2019) [D19], Buckley and Thoms (2012) [BT12], Dow AgroSciences (2010, 2011) [DA10 and DA11], MBTOC (2006, 2010, 2014, 2018) [MB6, MB10, MB14 and MB18], Prabhakaran et al. (2006) [P6], Cao et al. (2014) [C14], Widayanti et al. (2016) [W16], and Schwarz et al. (2011) [S11]

Region	Country	First year of start use	SF (%)	PT (%)
North America	USA [BT12, DA10-11, MB6-10-14-18]	before 2000	95	5
	Canada [DA10-11, MB6-10-14-18, P6]	2006	0	100
	Mexico [BT12, DA11, MB14-18]	2007	0	100
	Cuba [MB14]	2006	0	100
	Trinidad and Tobago [DA11, MB18]	2007	0	100
	Jamaica [MB14-18]	2010	0	100
Europe [MB6-10-14-18]	Italy [BT12, DA10-11, P6, S11]	2004	5	95
	Switzerland [DA10-11, P6]	2003	5	95
	Germany [BT12, DA10-11, P6, S11]	2004	5	95
	France [BT12, DA10-11, P6, S11]	2006	5	95
	UK [DA10-11, P6, S11]	2004	5	95
	Belgium [BT12, DA10, P6, S11]	2005	5	95
	Greece [BT12, DA10]	2009	5	95
	Spain [DA10-11, S11]	2007	5	95
	Ireland [DA10]	2007	0	100
	Portugal [DA10]	2010	5	95
	The Netherlands [BT12, DA10, S11]	2010	5	95
	Sweden [S11]	2004	5	95
	Austria [DA10, S11]	2004	5	95
	Turkey [BT12, DA10]	2009	5	95
	China [C14]	2014	0	100
	Thailand [MB14-18]	2009	0	100
Asia	Vietnam [MB14-18]	2009	0	100
	Japan [MB6-10-14-18]	before 2000	100	0
Australia	Australia [D19, BT12, DA10, P6]	2007	5	95
Other Countries	Egypt [MB14-18]	2010	0	100
	Indonesia [MB14-18, W16]	2010	0	100

$$d_{SO_2F_2}^{SF} = \text{pop}_{\text{wood housing}} \times \text{mask}_{\text{licensed countries}} \times \text{mask}_{\text{countries with termites}} \quad (1)$$

With $d_{SO_2F_2}^{SF}$, the spatial distribution of SF emissions (in km⁻²), $\text{pop}_{\text{wood housing}}$, the population density (CIESIN, 2018) considered for countries for which the residential buildings are built out of wood (in km⁻², FAO, 1971), $\text{mask}_{\text{licensed countries}}$, a grid of 0 or 1 (unitless) showing the countries where SO₂F₂ has been approved for SF (MBTOC, 2006, 2010, 2014, 2018; Dow AgroSciences, 2013) depending on the first year of start use (see Table 1), $\text{mask}_{\text{countries with termites}}$, a grid of 0 or 1 (unitless) showing areas, where we find termites (Ultimate Termite Control, <http://www.ultimatetermitecontrol.com/termite-infestation-probability-map/>) because SF by using SO₂F₂ is mainly associated with termite eradication.

$$d_{SO_2F_2}^{PT} = f_{\text{cropland}} \times d_{\text{grain production}} \times \text{mask}_{\text{licensed countries}} \quad (2)$$

With $d_{SO_2F_2}^{PT}$, the spatial distribution of PT emissions (in km⁻²), f_{cropland} , the cropland fraction (unitless, global ESRI grid based on the year 2000, Ramankutty, 2010), $d_{\text{grain production}}$, the global grain production (in

km⁻², FAO, 2020), mask_{licensed countries}, a grid of 0 or 1 (unitless) showing the countries where SO₂F₂ has been approved for PT (MBTOC, 2006, 2010, 2014, 2018; Dow AgroSciences, 2010, 2011), depending on the first year of start use (see Table 1). Note that by using the cropland fraction as a proxy, there is no spatial distinction of the types of crops. In addition, Equation 2 assigns SO₂F₂ emissions to all cropland regions but it may be possible that some of them do not involve SO₂F₂ fumigation.

To estimate the emissions magnitudes ($F_{SO_2F_2}^{\text{downscaling}}$), we allocate emissions to individual countries based on the spatial distribution of the SF and PT emissions, the AGAGE box model global emissions estimates, and the SF and PT partitioning (Table 1) as described in Equation 3.

$$F_{SO_2F_2}^{\text{downscaling}} = \left[\frac{\left(d_{SO_2F_2}^{\text{SF or PT}} \times F_{SO_2F_2}^{\text{top-down}} \times P \times 1e^6 \right)}{M_{SO_2F_2} \times 1e^6} \right] \times \frac{1e^{-7}}{3.15} \quad (3)$$

With $F_{SO_2F_2}^{\text{downscaling}}$, the downscaling estimate of SF or PT emissions (in mol m⁻² s⁻¹), $F_{SO_2F_2}^{\text{top-down}}$, the global emissions estimated by the AGAGE box model (in Gg yr⁻¹), P , the global SF and PT partitioning (unitless), $M_{SO_2F_2}$, the SO₂F₂ molar mass (in g mol⁻¹). The other numerical factors are for unit conversion. Where available, the data on SO₂F₂ consumption for each country are used to calculate the fumigant emissions. For North America, primarily California, the SO₂F₂ yearly total consumptions are provided by the Department of Pesticide Regulation (<https://www.cdpr.ca.gov/>) from 1995 to 2017 and extrapolated from 2017 to 2019. For Australia, the SO₂F₂ usage data are based on the total imports (Dunse et al., 2019). European emissions have been calculated by using the use estimate from the report on European F-gases (Schwarz et al., 2011) from 2006 to 2010 and extrapolated from 2000 to 2006 and from 2011 to 2019. To the best of our knowledge, there are no available data for SO₂F₂ usage in Asian countries. It should be noted that emissions may have occurred from regions of the world for which there is no authorized fumigation activity and such emissions would not be accounted for using the methods outlined here. The consumption is multiplied by the emissions factor $F = 2/3$ (Mühle et al., 2009) which is applied uniformly in space. The initial (proxy based as described in Equation 3) estimate is then rescaled according to this calculation.

Finally, the seasonality of the SO₂F₂ emissions is estimated. The emissions, which are determined on an annual basis, are distributed monthly over the year depending on the allocated seasonality. Structural fumigation releases are considered as continuous year-round emissions. Qualitative inspection of some AGAGE SO₂F₂ data suggests that SF might occur more often on long weekends (i.e., holidays), depending on the country, but to our knowledge there is no industry reference to support this variability. Seasonality is applied to PT fumigation depending on the region: in North America PT is assumed to occur uniformly during a 6-month season (from June to November inclusive), in Europe from June to December inclusive, in Australia from November to March inclusive, and in Asia from June to November inclusive (United States Department of Agriculture, International Production Assessment Division, <https://ipad.fas.usda.gov/og-amaps/cropcalendar.aspx>).

Regional emissions are calculated at monthly resolution and their spatial distribution is provided with a resolution of 0.352° × 0.234°, which corresponds to the horizontal resolution that has been used in several recent regional inverse modelling studies using the NAME model (the UK Met Office Numerical Atmospheric dispersion Modeling Environment, Jones et al., 2007 and Manning et al., 2011).

3. AGAGE SO₂F₂ Mole Fraction Data

AGAGE and its precursor programs provide a continuous record of in situ measurements of a comprehensive range of ODSs and GHGs since 1978 (Prinn et al., 2000, 2018). SO₂F₂ measurements have been made using the Medusa Gas Chromatography with Mass Spectrometry (GC-MS) system (Miller et al., 2008; Arnold et al., 2012). The SO₂F₂ measurement precision is 2%, calibrated relative to ambient air working standards, which have been prepared at the Scripps Institution of Oceanography (SIO). SO₂F₂ data are reported in the SIO-07 calibration scale (Prinn et al., 2000, 2018; Miller et al., 2008).

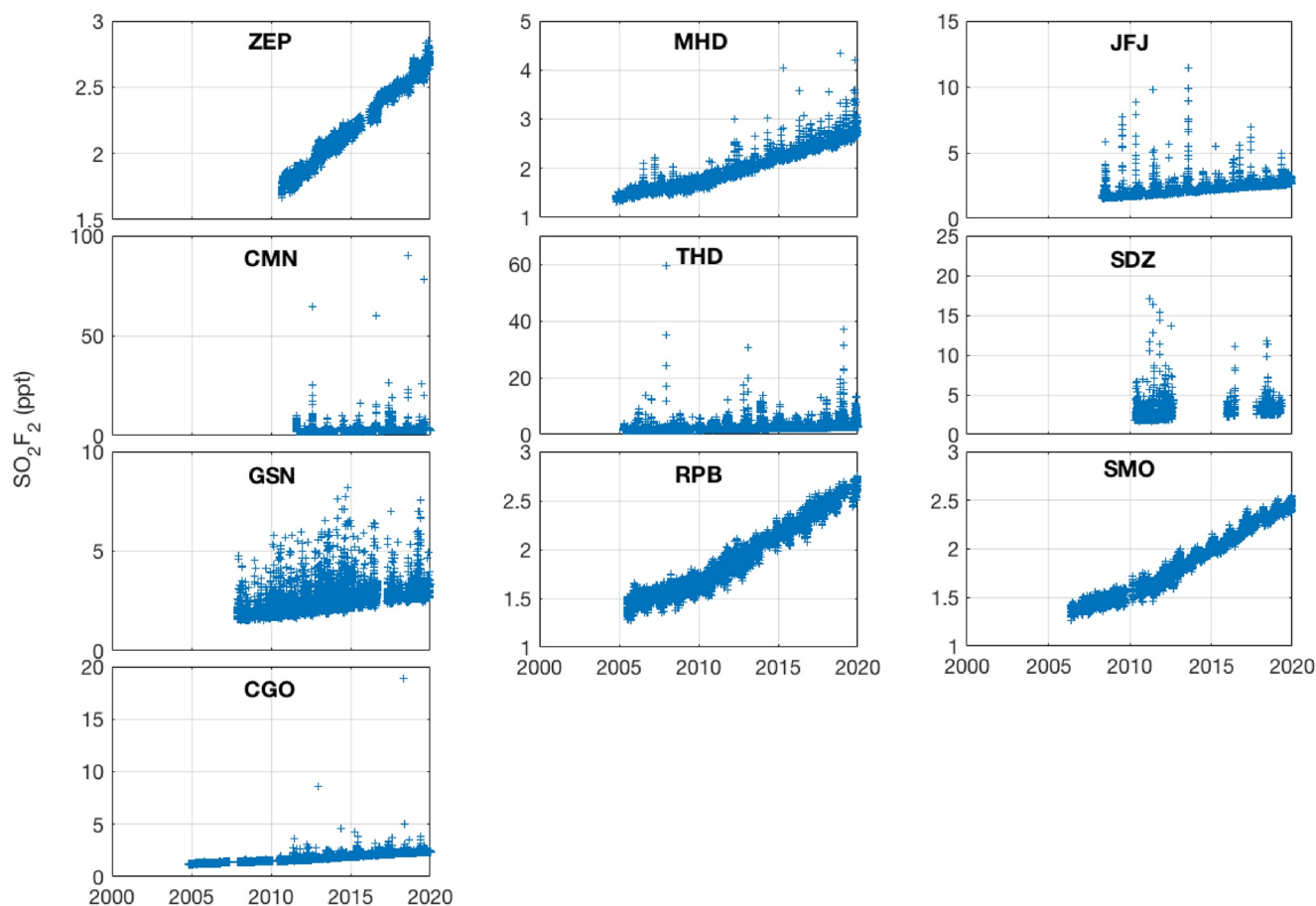


Figure 1. SO_2F_2 mole fractions (in ppt) observed at the Advanced Global Atmospheric Gases Experiment (AGAGE) sites (Zeppelin [ZEP], Mace Head [MHD], Jungfraujoch [JFJ], Monte Cimone [CMN], Trinidad Head [THD], Shangdianzi [SDZ], Gosan [GSN], Ragged Point [RPB], Cape Matatula [SMO], and Cape Grim [CGO]) from 2000 to 2019 inclusive.

SO_2F_2 was first discovered in ambient air at La Jolla in 2003, but we do not use this highly polluted data set due to close proximity to the San Diego urban area where SO_2F_2 is regularly used to fumigate houses for termite eradication (Mühle et al., 2009). Here, we use SO_2F_2 measurements starting in November 2004 at Cape Grim (CGO, Tasmania) and Mace Head (MHD, Ireland), in March 2005 at Trinidad Head (THD, California), in July 2005 at Ragged Point (RPB, Barbados), in May 2006 at Cape Matatula (SMO, Samoa), in November 2007 at Gosan (GSN, Korea), in April 2008 at Jungfraujoch (JFJ, Switzerland), in May 2010 at Shangdianzi (SDZ, China), in September 2010 at Zeppelin (ZEP, Norway), and in July 2011 at Monte Cimone (CMN, Italy). Only the measurement stations MHD, THD, RPB, SMO, and CGO were included in the box model inversions as they are the longest-running baseline stations. The other stations are used to qualitatively examine pollution events and other variability to inform the regional studies as discussed below, but are not used directly in the regional emissions estimation.

As a consequence of the use of SO_2F_2 to replace CH_3Br in the non-QPS sector beginning in 2003, in situ measurements (Figure 1) show a significant increase of SO_2F_2 global average mole fraction from 1.4 ppt in 2005 to 2.7 ppt in 2019. SO_2F_2 pollution events of upto 60 and 90 ppt are observed at THD and CMN, respectively. High mixing ratios are also recorded at JFJ (upto 12 ppt), GSN (15 ppt), SDZ (17 ppt), and CGO (18 ppt). Significant local sources or continental transport of high SO_2F_2 emissions are expected for those sites from their surrounding regions. Relatively low pollution events have been observed at MHD (upto 4 ppt), suggesting weaker and/or more distant sources compared to the sources driving pollution episodes at THD for example. Also, in contrast to THD, the measurements at SMO, RPB, and ZEP show mole fractions that are consistently close to the global background, with a few large pollution events, indicating generally background air with occasional impact of pollution from local sources of SO_2F_2 .

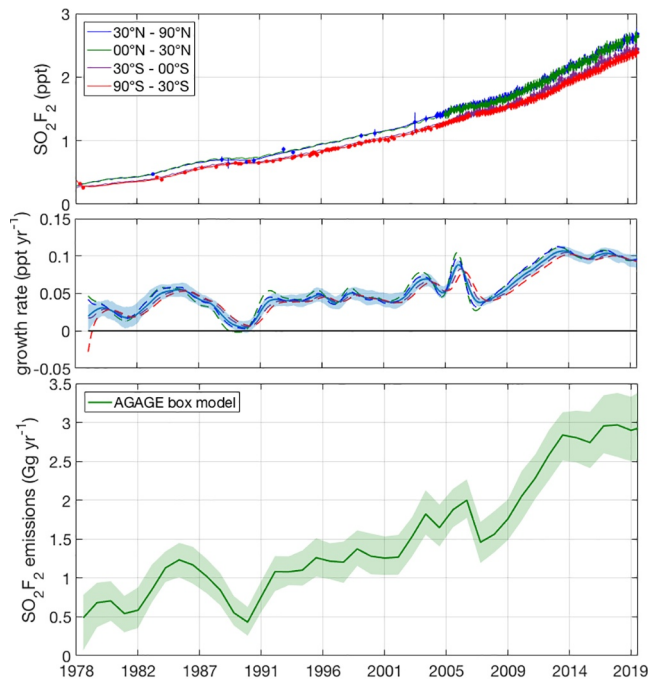


Figure 2. The semi-hemisphere averaged SO_2F_2 mole fractions (in ppt, upper plot), the global growth rate (in ppt yr^{-1} , middle plot, blue line) with the associated uncertainty (1-sigma, in shaded blue) and semi-hemispheric growth rates (dashed colored lines) and the inferred global emissions (in Gg yr^{-1} , bottom plot) with the associated uncertainty (1-sigma, in shaded green), estimated from the Advanced Global Atmospheric Gases Experiment (AGAGE) box model are presented for 1978–2019.

4. Results

4.1. SO_2F_2 Global Growth Rate and Global Emissions Derived from Atmospheric Data

The AGAGE measurements show a significant increase in the global annual mean SO_2F_2 mole fraction between 1978 and 2019 from 0.3 ± 0.02 to 2.5 ± 0.08 ppt (for gap-filling purposes, global averages are taken from the box model, into which measurements have been assimilated). The associated annual mean growth rate changed on average from 0.02 ± 0.02 ppt yr^{-1} to 0.09 ± 0.01 ppt yr^{-1} between 1978 and 2019 (following the method in Rigby et al., 2014). This growth rate can be seen to have increased most strongly between 2008 and 2014 with a maximum of 0.1 ± 0.01 ppt yr^{-1} in 2013. This can be explained by a rapid expansion of the use of SO_2F_2 during this period, especially as PT use began to be licensed in Asia (China, Thailand, Vietnam) and other countries (Jamaica, Turkey, Egypt, Indonesia). This trend corresponds to the increasing global SO_2F_2 emissions estimated by the inversion from 0.5 ± 0.4 Gg yr^{-1} in 1978 to 2.9 ± 0.4 Gg yr^{-1} in 2019 (Figure 2). There are two noteworthy reductions in emissions in the early 1990s (from 0.84 ± 0.2 Gg yr^{-1} in 1988 to 0.43 ± 0.2 Gg yr^{-1} in 1990) and in the mid-2000s (from 1.87 ± 0.3 Gg yr^{-1} in 2005 to 1.46 ± 0.3 Gg yr^{-1} in 2007), which might be explained by the economic crises that occurred during those periods. The numerical results for AGAGE measurements, the growth rate and the emissions are presented in the Supporting Information S2, S3, and S4, respectively.

4.2. Regional SO_2F_2 Emissions

Regional emissions estimates are shown in Figure 3. For all regions, the expansion of the PT use of SO_2F_2 is responsible for a significant part of the emissions increase during the period of the study. However, in North

America, the region with the highest average emissions throughout, SF remains the most important source of SO_2F_2 . The overall increase in emissions in North America, from 1.4 Gg yr^{-1} to 2.8 Gg yr^{-1} from 2000 to 2019, is primarily explained by SF in California and PT that started in Canada in 2006. Europe and Australia show small emissions related to SF with little year-to-year variation. Mainly because of the PT sector, SO_2F_2 emissions changed from 0 Gg yr^{-1} to 0.25 Gg yr^{-1} and from 0 Gg yr^{-1} to 0.1 Gg yr^{-1} between 2000 and 2019 in these regions, respectively. PT emissions in Asia became globally significant between 2008 and 2009 and by 2014, exceeded the Asian SF emissions that largely occurred in Japan. In this region, the total emissions increased from 0.09 Gg yr^{-1} to 0.54 Gg yr^{-1} between 2000 and 2019. In the other countries (Egypt and Indonesia), emissions increased in total from 0 Gg yr^{-1} to 0.12 Gg yr^{-1} between 2000 and 2019 only due to PT.

The proxy-based emissions estimate (following Equation 3) is rescaled based on the emissions calculated from consumption data when they are available. This could result in differences between global emissions from the top-down estimation and the total of the regional estimation. As shown in Figure 3, the total of the regional emissions is close to the upper uncertainty bound in the global top-down estimate until 2013. Subsequently, the total regional emissions exceed the top-down estimate. This could be explained by a potential overestimate of the SF emissions in the USA, where emissions are scaled from available SO_2F_2 consumption data in California. For the final 2 years, SO_2F_2 consumption data are extrapolated (see Section 2.2) which may lead to an overestimate of emissions. In addition, emissions from Asia are not rescaled since consumption data are not available. In this region, an emissions increase is calculated since 2007 for both SF and PT sectors. Without scaling with real data, the estimates in Asia could be biased and participate in the global overestimate. Note that the numerical results for PT, SF and their sum are presented in S5, S6, and S7 as well as the monthly emissions as S8 for the year 2019 in supporting information.

The spatial distribution of the SO_2F_2 emissions as an average of the 20-year period is presented in Figure 4. The SF emissions are primarily concentrated in California and Japan, with a maximum of 1.6×10^{-11} and

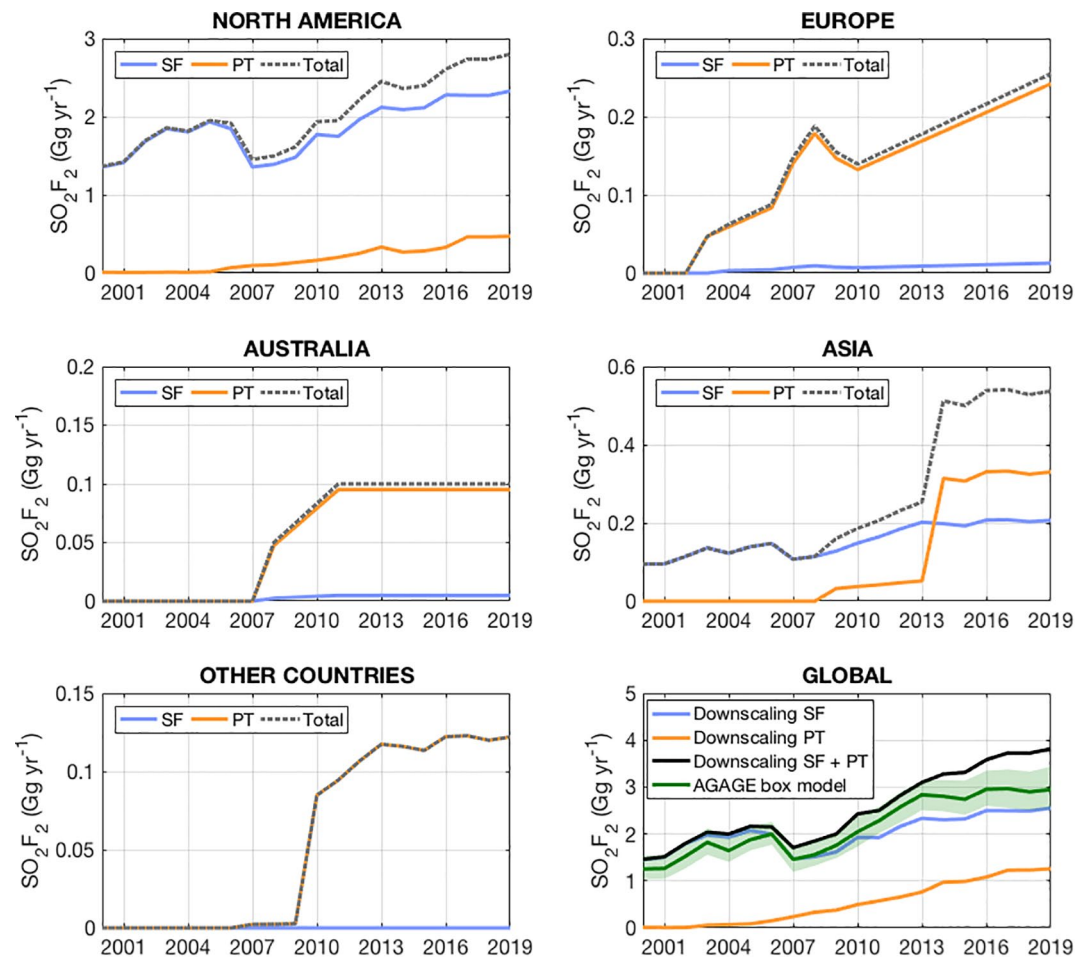


Figure 3. Annual average (2000–2019) SO_2F_2 emissions (Gg yr^{-1}) from structural fumigation (SF, blue), postharvest treatment (PT, orange), and the total (SF + PT, dashed grey) for North America (USA, Canada, Cuba, Mexico, Trinidad and Tobago, Jamaica), Europe (Italy, Switzerland, Germany, France, UK, Belgium, Greece, Spain, Ireland, Portugal, The Netherlands, Sweden, Austria, Turkey), Asia (China, Japan, Vietnam, Thailand), Australia, and Other Countries (Egypt, Indonesia). Global emissions for SF (in blue) and PT (in orange) and their sum (in black) are presented and compared to the Advanced Global Atmospheric Gases Experiment (AGAGE) box model results (in green) with the related uncertainty (1-sigma) in shaded green.

$2.4 \times 10^{-12} \text{ mol m}^{-2} \text{ s}^{-1}$, respectively, and to a lesser extent in the eastern part of the USA, south west Europe, and Turkey with a maximum of 1.6×10^{-12} , 2.4×10^{-14} , and $6.3 \times 10^{-14} \text{ mol m}^{-2} \text{ s}^{-1}$, respectively.

The PT emissions are mainly distributed in Canada (upto $1.5 \times 10^{-14} \text{ mol m}^{-2} \text{ s}^{-1}$), California ($3.3 \times 10^{-13} \text{ mol m}^{-2} \text{ s}^{-1}$), Mexico ($2.1 \times 10^{-14} \text{ mol m}^{-2} \text{ s}^{-1}$), Cuba ($1.7 \times 10^{-14} \text{ mol m}^{-2} \text{ s}^{-1}$), western Europe ($1.2 \times 10^{-13} \text{ mol m}^{-2} \text{ s}^{-1}$), Indonesia ($2 \times 10^{-14} \text{ mol/m}^2/\text{s}$), Thailand ($2 \times 10^{-14} \text{ mol/m}^2/\text{s}$), southern mainland Australia ($3.3 \times 10^{-14} \text{ mol m}^{-2} \text{ s}^{-1}$), and to a lesser extent eastern USA, China, and Tasmania with a maximum of 1×10^{-14} , 1×10^{-14} , and $5 \times 10^{-15} \text{ mol m}^{-2} \text{ s}^{-1}$, respectively. This is mainly dependent on the crop fraction and the grain production volumes. Note that the averages for three different periods (2000–2007, 2008–2014, 2015–2019) are presented in the Supporting Information (Supporting Information S9, S10, S11, and S12).

This SO_2F_2 emissions estimation in high spatial resolution could be used as inputs to future regional inversions. However, such an approach would likely need to be able to account for the possibility that emissions could be highly episodic, particularly for SF, where emissions may be focused on periods, such as holidays, where buildings are expected to be vacant.

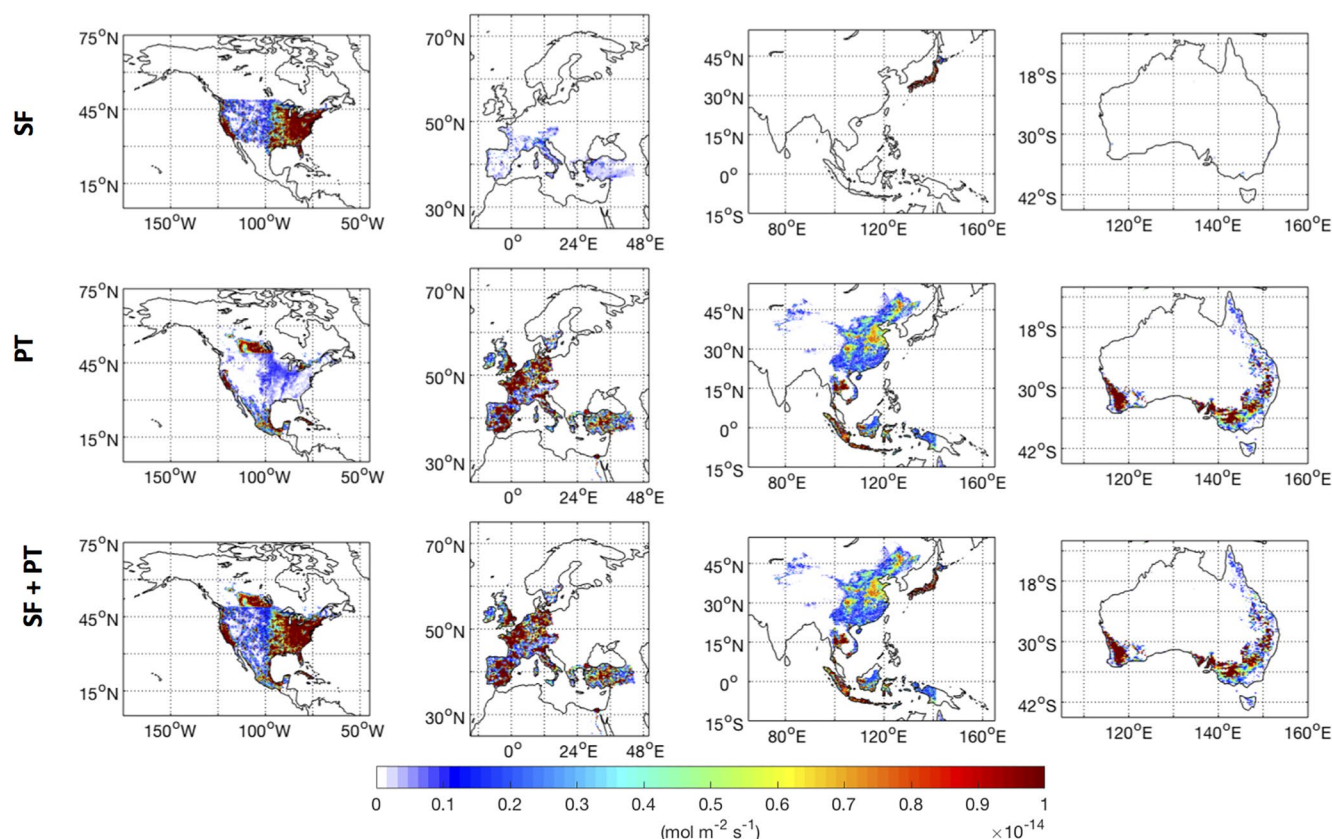


Figure 4. Average SO_2F_2 emissions (2000–2019, mol $\text{m}^{-2} \text{s}^{-1}$) from the downscaling approach at $0.352^\circ \times 0.234^\circ$ horizontal resolution for structural fumigation (SF), postharvest treatment (PT), and their sum (SF + PT), in North America (USA, Canada, Cuba, Mexico, Trinidad and Tobago, Jamaica), Europe (Italy, Switzerland, Germany, France, UK, Belgium, Greece, Spain, Ireland, Portugal, The Netherlands, Sweden, Austria, Turkey) + Egypt, Asia (China, Japan, Vietnam, Thailand) + Indonesia, and Australia.

5. Summary

We present an update of the SO_2F_2 global emissions based on the AGAGE box model inversions from 1978 to 2019. The calculations are based on AGAGE in situ observations that show a significant increase of the SO_2F_2 mole fraction in the global atmosphere in response to the Montreal Protocol mandated phase-down of CH_3Br use. Emissions are correspondingly estimated to increase from $0.5 \pm 0.4 \text{ Gg yr}^{-1}$ in 1978 to $2.9 \pm 0.4 \text{ Gg yr}^{-1}$ in 2019. For the first time, the SO_2F_2 emissions were estimated from 2000 to 2019 on regional scales for countries in North America (USA, Canada, Mexico, Cuba, Trinidad and Tobago, Jamaica), Europe (Italy, Switzerland, Germany, France, UK, Belgium, Greece, Spain, Ireland, Portugal, The Netherlands, Sweden, Austria, Turkey), Asia (China, Japan, Vietnam, Thailand), Australia, and for individual countries where use has been identified (Egypt, Indonesia). These regional estimates are based on consumption reports and a downscaling of global emissions, based on proxies that define the spatial distribution, the magnitude and the seasonality of the emissions which are specific to each sector. Results show that the increase in emissions is partly due to the expansion of the use of SO_2F_2 for PT, although SF remains the main source of the gas emissions in North America, which is the major global emitter. An estimate of the spatial distribution of total, SF and PT SO_2F_2 emissions at high resolution is provided monthly over the 20-year period. This spatial distribution could be used as a prior estimate of emissions in future top-down inversions of SO_2F_2 data at regional scales. It will be important to constrain regional budgets in the future, as SO_2F_2 emissions are expected to continue to increase in the long term because of a growing global demand for postharvest treatment and structural fumigation.

Data Availability Statement

AGAGE measurements that were used for this research are available in these in-text data citation references: Prinn, Weiss, Fraser, et al., 2000, 2018 (https://agage2.eas.gatech.edu/data_archive/). Observations from archived air samples used for this research are included in Mühle et al., 2009, their Section 2.3. Note that the spatial distribution of total, SF and PT SO₂F₂ emissions over the 20-year period is available from <https://osf.io/b6mwr/>.

Acknowledgments

The authors thank the station staff (AGAGE and others) for ensuring high quality instrument performance, providing state-of-the-art, and reliable data. Funding for this work, as well as operation of the AGAGE instruments at Mace Head, Trinidad Head, Cape Matatula, Ragged Point, and Cape Grim, were from the National Aeronautics and Space Administration (NASA) (grants NAG5-12669, NNX07AE89G, NNX11AF17G and NNX16AC98G to MIT and grants NNX07AE87G, NNX-07AF09G, NNX11AF15G, and NNX-11AF16G to SIO), the Department for Business, Energy and Industrial Strategy (BEIS, UK) contract 1028/06/2015 in support of Mace Head and the National Oceanic and Atmospheric Administration (NOAA, USA), contract RA-133-R15-CN-0008 to the University of Bristol in support of Ragged Point, Barbados, the Commonwealth Scientific and Industrial Research Organization (CSIRO Australia), the Bureau of Meteorology (Australia), the Department of Agriculture, Water and the Environment (Australia). Support for the Jungfraujoch measurements is provided by the Swiss National Programs HALCLIM and CLIMGAS-CH (Swiss Federal Office for the Environment, FOEN) and by the International Foundation High Altitude Research Stations Jungfraujoch and Gornergrat (HFSJG). Support for Monte Cimone operation is provided by the National Research Council (CNR) of Italy and the Italian Ministry of Education, University and Research, through the Project of National Interest "Nextdata". Support for Shangdianzi measurements is provided by the China Meteorological Administration Operational Funding and the National Nature Science Foundation of China (41575114). Sunyoung Park (and the Gosan AGAGE station) is supported by the National Research Foundation of Korea (NRF) grant funded by the Korea government (MSIT) (No. 2020R1A2C3003774). SO₂F₂ measurements at Zeppelin are supported by the Norwegian Environment Agency. Anita Ganesan was supported by a UK Natural Environment Research Council Fellowship (NE/L010992/1). The SIO group also thanks Dow AgroSciences and Douglas Products for their long-term support of SO₂F₂ measurements in the global atmosphere.

References

- Arnold, T., Mühle, J., Salameh, P. K., Harth, C. M., Ivy, D. J., & Weiss, R. F. (2012). Automated measurement of nitrogen trifluoride in ambient air. *Analytical Chemistry*, 84, 4798–4804. <https://doi.org/10.1021/ac300373e>
- Buckley, S., & Thoms, E. (2012). Current status of ProFume® gas fumigant for disinfestation of commodities. In S. Navarro, H. J. Banks, D. S. Jayas, C. H. Bell, R. T. Noyes, A. G. Ferizli, M. Emekci, A. A. Isikber, & K. Alagusundaram (Eds.), *Proceedings of the international conference on controlled atmosphere and fumigation in stored products* (pp. 241–246). Antalya, Turkey: ARBER Professional Congress Services.
- Burkholder, J. B., Sander, S. P., Abbott, J., Barker, J. R., Huie, R. E., Kolb, C. E., et al. (2015). *Chemical kinetics and photochemical data for use in atmospheric studies, evaluation No. 18*. Pasadena, CA: JPL Publication 15-10, Jet Propulsion Laboratory. <http://jpldataeval.jpl.nasa.gov>
- Cao, A., Guo, M., Yan, D., Mao, L., Wang, Q., Li, Y., et al. (2014). Evaluation of sulfuryl fluoride as a soil fumigant in China. *Pest Management Science*, 70, 219–227. <https://doi.org/10.1002/ps.3535>
- Carpenter, L. J., Reimann, S., Burkholder, J. B., Clerbaux, C., Hall, B. D., Hossaini, R., et al. (2014). Ozone-depleting substances (ODSs) and other gases of interest to the montreal protocol. *Scientific assessment of ozone depletion: 2014, global ozone research and monitoring project: Report no. 55* (p. 88). Geneva, Switzerland: World Meteorological Organization.
- CIESIN. (2018). *Gridded population of the world, version 4 (GPWv4): Population density, revision 11*. Palisades, NY: NASA Socioeconomic Data and Applications Center (SEDAC). <https://doi.org/10.7927/H49C6VHW>
- Cunnold, D. M., Prinn, R. G., Rasmussen, R. A., Simmonds, P. G., Alyea, F. N., Cardelino, C. A., et al. (1983). The atmospheric lifetime experiment: 3. Lifetime methodology and application to three years of CFC₁₃ data. *Journal of Geophysical Research*, 88, 8379–8400. <https://doi.org/10.1029/jc088ic13p08379>
- Dillon, T. J., Horowitz, A., & Crowley, J. N. (2008). The atmospheric chemistry of sulphuryl fluoride, SO₂F₂. *Atmospheric Chemistry and Physics*, 8, 1547–1557. <https://doi.org/10.5194/acp-8-1547-2008>
- Dow AgroSciences. (2010). *Regulatory update for ProFume® gas fumigant, methyl bromide and alternatives in food plants: Past, present, and future "practical pest management methods for 2010 and beyond"*. <https://www.grains.k-state.edu/spirel/docs/conferences/mb-alternatives/presentation/dave%20barnekow.pdf>
- Dow AgroSciences. (2011). *ProFume® gas fumigant update: Diverse uses for commodity protection*. <http://www.fumigaciya.ru/sites/default/files/public/page/2011-09/15/profume.pdf>
- Dow AgroSciences. (2013). *General information on Vikane gas fumigant* (p. 8). U01-069-152 (06/13) DAS 010-70087.
- Dunse, B. L., Derek, N., Fraser, P. J., Krummel, P. B., & Steele, L. P. (2019). *Australian and global HFC, PFC, sulfur hexafluoride nitrogen trifluoride and sulfuryl fluoride emissions* (p. 33). Aspendale, Australia: Australian Government Department of the Environment and Energy, CSIRO Oceans and Atmosphere.
- Engel, A., Rigby, M., Burkholder, J. B., Fernandez, R. P., Froidevaux, L., Hall, B. D., et al. (2018). Update on ozone-depleting substances (ODSs) and other gases of interest to the Montreal protocol. *Scientific assessment of ozone depletion: 2018, global ozone research and monitoring project: Report No. 58*. Geneva, Switzerland: World Meteorological Organization.
- Fang, X., Yao, B., Vollmer, M. K., Reimann, S., Liu, L., Chen, L., et al. (2019). Changes in HCFC Emissions in China During 2011–2017. *Geophysical Research Letters*, 46(16), 10034–10042. <https://doi.org/10.1029/2019gl083169>
- FAO. (1971). An international review of forestry and forest products. In *World consultation on the use of wood in housing* (pp. 101–102). Food and Agriculture Organization of the United Nations.
- FAO. (2020). *FAOSTAT*. <http://www.fao.org/faostat/fr/#data/QC>
- Hobbs, J. P., & Hart, J. J. (2004). *Plasma cleaning gas with lower global warming potential than SF6, report*. Allentown, PA: Air Products and Chemicals, Inc.
- Jones, A., Thomson, D., Hort, M., & Devenish, B. (2007). The U.K. Met office's next-generation atmospheric dispersion model, NAME III. *Air pollution modeling and its applications Xvii* (17, 580–589). https://doi.org/10.1007/978-0-387-68854-1_62
- Kórhé, O., Rikker, T., Molnár, G., Mahara, B. M., Torkos, K., & Borossay, J. (1997). Study of decomposition of sulphur hexafluoride by gas chromatography/mass spectrometry. *Rapid Communications in Mass Spectrometry*, 11, 1643–1648. [https://doi.org/10.1002/\(SICI\)1097-0231\(19971015\)11:15<1643:AID-RCM14>3.0.CO;2-C](https://doi.org/10.1002/(SICI)1097-0231(19971015)11:15<1643:AID-RCM14>3.0.CO;2-C)
- Manning, A. J., O'Doherty, S., Jones, A. R., Simmonds, P. G., & Derwent, R. G. (2011). Estimating UK methane and nitrous oxide emissions from 1990 to 2007 using an inversion modeling approach. *Journal of Geophysical Research*, 116, D02305. <https://doi.org/10.1029/2010jd014763>
- MBTOC. (2006). *Report of the methyl bromide technical options committee. 2006 assessment* (p. 475). Nairobi: UNEP. ozone.unep.org
- MBTOC. (2010). *Report of the methyl bromide technical options committee. 2006 assessment* (p. 387). Nairobi: UNEP. ozone.unep.org
- MBTOC. (2014). *Report of the methyl bromide technical options committee. 2006 assessment* (p. 277). Nairobi: UNEP. ozone.unep.org
- MBTOC. (2018). *Report of the methyl bromide technical options committee. 2006 assessment* (p. 139). Nairobi: UNEP. ozone.unep.org
- Miller, B. R., Weiss, R. F., Salameh, P. K., Tanhua, T., Grealley, B. R., Mühle, J., & Simmonds, P. G. (2008). Medusa: A sample preconcentration and GC/MS detector system for in situ measurements of atmospheric trace halocarbons, hydrocarbons, and sulfur compounds. *Analytical Chemistry*, 80, 1536–1545. <https://doi.org/10.1021/ac702084k>
- Mühle, J., Huang, J., Weiss, R. F., Prinn, R. G., Miller, B. R., Salameh, P. K., et al. (2009). Sulfuryl fluoride in the global atmosphere. *Journal of Geophysical Research*, 114, D05306. <https://doi.org/10.1029/2008JD011162>
- Mühle, J., Trudinger, C. M., Western, L. M., Rigby, M., Vollmer, M. K., Park, S., et al. (2019). Perfluorocyclobutane (PFC-318, c-C4F8) in the global atmosphere. *Atmospheric Chemistry and Physics*, 19, 10335–10359. <https://doi.org/10.5194/acp-19-10335-2019>

- O'Doherty, S. J., Simmonds, P. G., Cunnold, D. M., Wang, R. H. J., Sturges, W. T., Fraser, P. J., et al. (2001). In situ chloroform measurements at advanced global atmospheric gases experiment atmospheric research stations from 1994 to 1998. *Journal of Geophysical Research*, 106, 20429–20444.
- Papadimitriou, V. C., Portmann, R. W., Fahey, D. W., Mühle, J., Weiss, R. F., & Burkholder, J. B. (2008). Experimental and theoretical study of the atmospheric chemistry and global warming potential of SO₂F₂. *The Journal of Physical Chemistry A*, 112, 12657–12666. <https://doi.org/10.1021/jp806368u>
- Prabhakaran, S. (2006). Commercial performance and global development status of profume gas fumigant. *PS6-19-6259, 9th international working conference on stored product protection*. São Paulo, Brazil: Brazilian Post-harvest Association.
- Prinn, R. G., Weiss, R. F., Arduini, J., Arnold, T., DeWitt, H. L., Fraser, P. J., et al. (2018). History of chemically and radiatively important atmospheric gases from the advanced global atmospheric gases experiment (AGAGE). *Earth System Science Data*, 10, 985–1018. <https://doi.org/10.5194/essd-10-985-2018>
- Prinn, R. G., Weiss, R. F., Fraser, P. J., Simmonds, P. G., Cunnold, D. M., Alyea, F. N., et al. (2000). A history of chemically and radiatively important gases in air deduced from ALE/GAGE/AGAGE. *Journal of Geophysical Research*, 105, 17751–17792. <https://doi.org/10.1029/2000JD900141>
- Ramankutty, N., Evan, A. T., Monfreda, C., & Foley, J. A. (2010). *Global agricultural lands: Croplands, 2000*. Palisades, NY: NASA Socioeconomic Data and Applications Center (SEDAC). <https://doi.org/10.7927/H4C8276G>
- Rigby, M., Ganesan, A. L., & Prinn, R. G. (2011). Deriving emissions time series from sparse atmospheric mole fractions. *Journal of Geophysical Research*, 116, D08306. <https://doi.org/10.1029/2010JD015401>
- Rigby, M., Park, S., Saito, T., Western, L. M., Redington, A. L., Fang, X., et al. (2019). Increase in CFC-11 emissions from eastern China based on atmospheric observations. *Nature*, 569, 546–550. <https://doi.org/10.1038/s41586-019-1193-4>
- Rigby, M., Prinn, R. G., O'Doherty, S., Miller, B. R., Ivy, D., Mühle, J., et al. (2014). Recent and future trends in synthetic greenhouse gas radiative forcing. *Geophysical Research Letters*, 41, 2623–2630. <https://doi.org/10.1002/2013GL059099>
- Rigby, M., Prinn, R. G., O'Doherty, S., Montzka, S. A., McCulloch, A., Harth, C. M., et al. (2013). Re-evaluation of the lifetimes of the major CFCs and CH₃CCl₃ using atmospheric trends. *Atmospheric Chemistry and Physics*, 13, 2691–2702. <https://doi.org/10.5194/acp-13-2691-2013>
- Say, D., Ganesan, A. L., Lunt, M. F., Rigby, M., O'Doherty, S., Harth, C., et al. (2019). Emissions of halocarbons from India inferred through atmospheric measurements. *Atmospheric Chemistry and Physics*, 19, 9865–9885. <https://doi.org/10.5194/acp-19-9865-2019>
- Schwarz, W., Gschrey, B., Leisewitz, A., Herold, A., Gores, S., Papst, I., et al. (2011). *Preparatory study for a review of Regulation (EC) No 842/2006 on certain fluorinated greenhouse gases, final report and annexes to the final report*. https://ec.europa.eu/clima/sites/clima/files/f-gas/docs/2011_study_en.pdf
- Spivakovsky, C. M., Logan, J. A., Montzka, S. A., Balkanski, Y. J., Foreman-Fowler, M., Jones, D. B. A., et al. (2000). Three-dimensional climatological distribution of tropospheric OH: Update and evaluation. *Journal of Geophysical Research*, 105, 8931–8980. <https://doi.org/10.1029/1999JD901006>
- Widayanti, S., Harahap, I. S., Rivai, M., Asnan, T. A. W., & Wibawa, K. A. (2016). Efficacy of sulfuryl fluoride against major insect pests of stored commodities in Indonesia. In S. Navarro, D. S. Jayas, & K. Alagusundaram (Eds.), *Proceedings of the 10th international conference on controlled atmosphere and fumigation in stored products (CAF2016)*, CAF permanent committee secretariat (pp. 188–191). Winnipeg, Canada.
- Yvon-Lewis, S. A., & Butler, J. H. (2002). Effect of oceanic uptake on atmospheric lifetimes of selected trace gases. *Journal of Geophysical Research*, 107(D20), 4414. <https://doi.org/10.1029/2001JD001267>

References from the Supporting Information

- DPR. (2006). *Summary of pesticide use report data*. California Department Of Pesticide Regulation. <https://www.cdpr.ca.gov/docs/pur/purmain.htm>
- DPR. (2017). *Summary of pesticide use report data*. California Department of Pesticide Regulation. https://www.cdpr.ca.gov/docs/pur/pur17rep/17_pur.htm
- Noppe, H., Buckley, S., & Ruebsamen, B. (2012). *Possibilities of PROFUME gas fumigant for the commercial fumigation of stored cocoa beans in EU* (pp. 379–383).
- Walse, S., Leesch, J. G., & Tebbets, S. (2009). Ovicidal efficacy of sulfuryl fluoride to stored-product pests of dried fruit. In G. L. Obenauf (Ed.), *Proceedings of the annual international research conference on methyl bromide alternatives and emission reduction*, 9–12 November in San Diego, CA, USA, MBAO conference (pp. 601–602). www.mbao.org